CLIMATE CHANGE

The weakening summer circulation in the Northern Hemisphere mid-latitudes

Dim Coumou,[1]* Jascha Lehmann,[1,2] Johanna Beckmann[1,2]

Rapid warming in the Arctic could influence mid-latitude circulation by reducing the poleward temperature gradient. The largest changes are generally expected in autumn or winter, but whether significant changes have occurred is debated. Here we report significant weakening of summer circulation detected in three key dynamical quantities: (i) the zonal-mean zonal wind, (ii) the eddy kinetic energy (EKE), and (iii) the amplitude of fast-moving Rossby waves. Weakening of the zonal wind is explained by a reduction in the poleward temperature gradient. Changes in Rossby waves and EKE are consistent with regression analyses of climate model projections and changes over the seasonal cycle. Monthly heat extremes are associated with low EKE, and thus the observed weakening might have contributed to more persistent heat waves in recent summers.

Enhanced warming in the Arctic could change circulation patterns in the mid-latitudes by reducing the pole–to–mid-latitude thermal gradient (*1*–*3*). This hypothesis, which was first proposed in the 1970s based on model experiments (*4*, *5*), has recently received considerable attention due to rapid observed warming in the Arctic (*6*–*9*), associated with a decline in sea ice and other factors (*1*, *3*, *10*).

Most studies addressing the link between Arctic change and mid-latitude weather have focused on winter circulation. The extra heat stored in the ocean owing to sea-ice loss is released into the atmosphere by late autumn or early winter, when air temperatures drop below sea surface temperatures. Consequently, the largest absolute increases in Arctic geopotential height have been detected in autumn and winter (*6*), consistent with climate model simulations (*11*). Autumn has, at least in the western half of the hemisphere, also seen a reduction in the zonal-mean flow (*6*, *12*). This might cause a slowdown in wave propagation (*6*), but the results are sensitive to the exact metrics used to describe waves (*12*, *13*). Thus, whether observed changes in geopotential height have affected mid-latitude Rossby waves remains disputed (*6*, *12*–*14*).

We studied changes in mid-latitude circulation in boreal summer instead. Although the oceanic heat flux is smaller in this season (*11*), Arctic amplification has reduced the pole–to–mid-latitude temperature gradient (*1*), and Arctic geopotential heights have increased (*6*). These changes are likely to be related to the earlier loss of snow cover over land and increased Arctic sea surface temperatures where sea ice has been lost (*7*). In recent summers, mid-latitude circulation has been dominated by a negative Arctic Oscillation index; i.e., anomalously small pressure differences between mid- and high-latitudes (*7*, *15*–*17*). Moreover, several recent heat waves, such as in Russia in 2010, were associated with persistent hemispheric circulation patterns (*15*, *16*, *18*).

Generally, the large-scale mid-latitude atmosphere dynamics [supplementary materials (SM) text S4] are characterized by (i) fast-traveling free Rossby waves (the so-called synoptic transients) with zonal wave numbers typically larger than 6, and (ii) quasi-stationary Rossby waves with normally smaller wave numbers as a response to quasi-stationary diabatic and orographic forcing (*15*, *19*–*21*). We focus on the first. These waves are associated with synoptic-scale cyclones (storms) and anticyclones (high-pressure systems), which form the storm track regions in the mid-latitudes. They have a relatively fast phase velocity (i.e., eastward propagation) and cause weather variability on time scales of less than a week. Typically, the intensity of synoptic-scale wave (or eddy) activity is estimated by applying a 2.5- to 6-day bandpass filter to high-resolution wind field data (*22*–*24*). This way, the total eddy kinetic energy (EKE) is extracted, which is a measure of the interplay between the intensity and frequency of high- and low-pressure systems associated with fast-traveling Rossby waves. Due to the quasi-stationary nature of thermally and orographically forced waves, as analyzed in related studies (*15*, *16*, *25*, *26*), they have lower frequencies and are thus excluded from our EKE computations (SM text S4).

We calculated EKE in the Northern Hemisphere from daily ERA-Interim wind fields (*27*), using a 2.5- to 6-day bandpass filter [see (*23*, *24*, *28*)]. We limited our analysis to the satellite-covered period (after 1979) to minimize the effects of changes in the observing system (SM text S2). The 1979–2013 period has seen a steady decline in summertime EKE (Fig. 1A). This decline is statistically significant at the 1% level and observed at all pressure levels, with the strongest relative changes in the lower to mid-troposphere (figs. S1 to S4 and table S1). Moreover, it occurs over the full hemisphere and over all relevant latitudes (fig. S5). The observed changes are thus not due to a north-south shift of storm tracks but due to a spatially homogeneous weakening. Other reanalysis products give similar results (figs. S6 to S11). For the other seasons, trends in EKE are also downward, but none are significant (figs. S12 to S17).

The decline in summer EKE is accompanied by a long-term decline in the zonal-mean zonal wind (U, Fig. 1B). Again, this weakening of the

[1]Potsdam Institute for Climate Impact Research, Earth System Analysis, 14412 Potsdam, Germany. [2]University of Potsdam, Potsdam, Germany.
*Corresponding author. E-mail: coumou@pik-potsdam.de

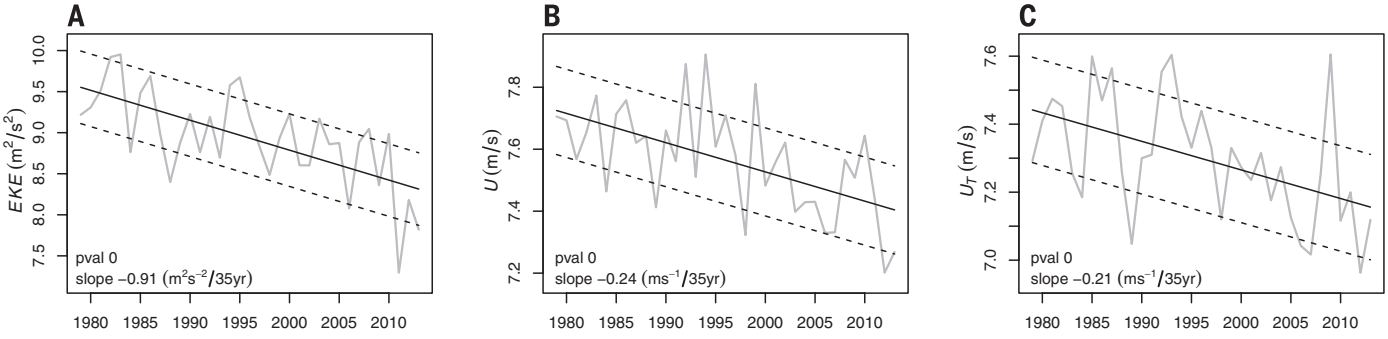

Fig. 1. Weakening summer circulation in the mid-latitudes. Absolute changes in (**A**) EKE, (**B**) zonal wind U, and (**C**) thermal wind U_T over 1979–2013 in summer (June, July, and August). Variables are calculated at 500 mb and averaged over 35°N to 70°N and all longitudes, with gray lines plotting observations, solid black lines the linear trend, and dashed black lines the ±1 residual SE range. Slope and P values for the trend estimates are given in the panels.

zonal flow is seen at all altitudes and in different reanalysis products (figs. S1 to S4 and S6 to S10). The long-term weakening of the zonal flow is consistent with the decline in the pole-to-mid-latitude thermal gradient. This is shown by the downward trend of similar magnitude in thermal wind U_T (Fig. 1C), which depends on changes in the temperature gradient only (eq. S2).

Although the relative decrease in EKE has been by 8 to 15% (depending on pressure level) over the 35-year period, the zonal flow weakened by only 4 to 6% (table S1). A similar relationship between changes in EKE and zonal flow is seen in future projections of CMIP5 (Coupled Model Intercomparison Project Phase 5) climate models. Under a high-emission scenario, summer EKE declines primarily because of decreased vertical wind shear associated with weakening of the zonal-mean flow (*24*). This projected reduction in EKE is spatially homogeneous, similar to the observed changes. Regression analysis of future changes in EKE and in zonal flow for individual CMIP5 models reveals a significant linear relationship (Fig. 2). The regression slope of ~1.4 indicates that a reduction in U is associated with a more pronounced reduction in EKE. This is seen at all pressure levels, with the regression slope increasing with altitude (fig. S18). Increased static stability plays a role as well (*24*, *29*), which explains why the linear regression crosses the y axis at negative values: Even for zero change in U, increased static stability in a warmer climate causes EKE to decline. The observed relative changes in U and EKE over the past 35 years map reasonably well on the regression of projected future changes (Fig. 2).

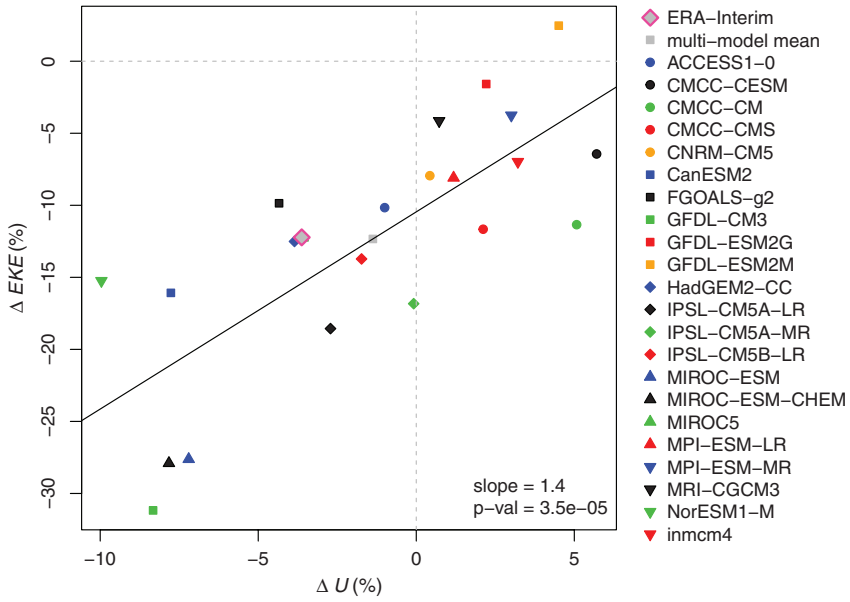

Fig. 2. Relationship between relative changes (Δ) in EKE and *U* in climate model projections. The percentage change in the future (2081–2100, under scenario RCP8.5) relative to 1981–2000 for individual CMIP5 climate models is shown. Both quantities are averaged over 35°N to 70°N, all longitudes, and over 850 to 250 mb (mass-weighted). The solid black line shows the linear fit, with slope and *P* value given at lower right. Relative changes in EKE and *U* in the ERA-Interim data are given for the 1979–2013 period.

The pronounced weakening in EKE should also be reflected in changed wave characteristics. To test this, we applied spectral analysis to the north-south wind component v in daily wind field data and calculated amplitude (A_v), phase speed, and period for wave numbers 1 to 15 (SM text S1.1). This way, fast-moving and quasi-stationary waves are not explicitly separated (as in EKE by using bandpass filtering), but because we used daily data, the mean wave amplitudes are dominated by fast-moving waves (SM text S4). The results are therefore comparable with EKE. We determined the wave quantities for the north-south wind component v averaged over 35°N to 70°N, and A_v thus reflects wind speeds with units of meters per second.

The amplitudes of all wave numbers except 7 have declined, with significant reductions in waves 1, 3, 4, 6, and 10 and in the mean amplitude of all waves. These changes are robust, detected in ERA-Interim and NCEP-NCAR (National Centers for Environmental Prediction–National Center for Atmospheric Research) data and for different pressure levels, with the strongest changes in the mid-troposphere (Fig. 3A and fig. S19). This vertical pattern is consistent with the more pronounced changes in EKE, U (table S1), and poleward temperature gradient (*1*) in the lower troposphere. The mean amplitude declined by –5% over 1979–2013 (Fig. 3A), similar to the relative reduction in U (fig. S1B). This is consistent with the seasonal correlation of these quantities (Fig. 3B), which shows that, to a first order, daily anomalies in mean A_v scale with those in U. This positive correlation is expected as daily wind fields, and thus A_v, will be dominated by transient eddies, because their kinetic energy is nearly an order of magnitude larger than that of quasi-stationary waves (*30*). Transient eddies are not only forced by the zonal flow via vertical shear (and thus baroclinicity) but can also accelerate it via the eddy-driven jet (*1*, *31*), explaining the positive correlation between U and A_v (SM text S4). The reduction of –5% in mean wind speed (A_v) implies a –10% reduction

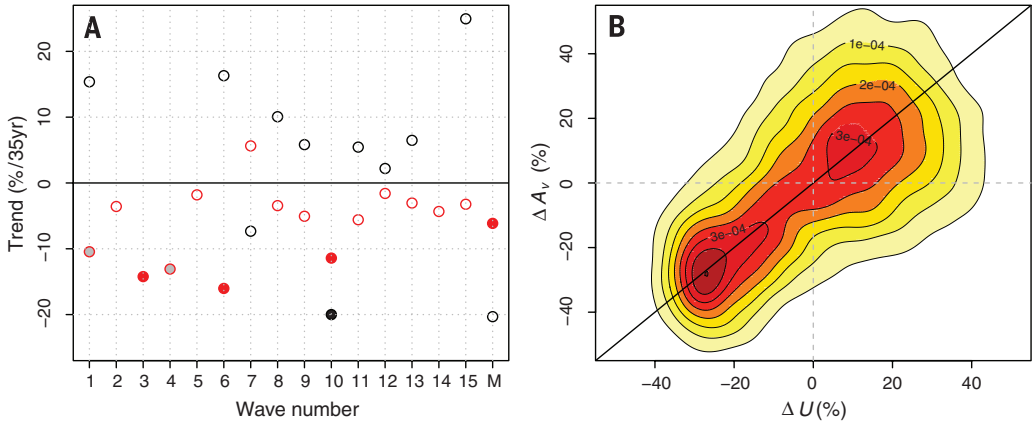

Fig. 3. (**A**) Trends in planetary wave amplitudes (A_v, red) and phase speed (black) at 500 mb in summer for wave numbers 1 to 15 and for the mean of all waves (*M*) in units of percentage change per 35 years; i.e., the period 1979–2013. Solid circles indicate 5% statistical significance, gray-filled circles indicate 10% statistical significance, and open circles are not significant. (**B**) Two-dimensional probability density distribution of daily deviations (in percentage change of their annual mean climatological values) of the zonal flow and the mean amplitude of waves 1 to 15. The bisecting line is shown in black.

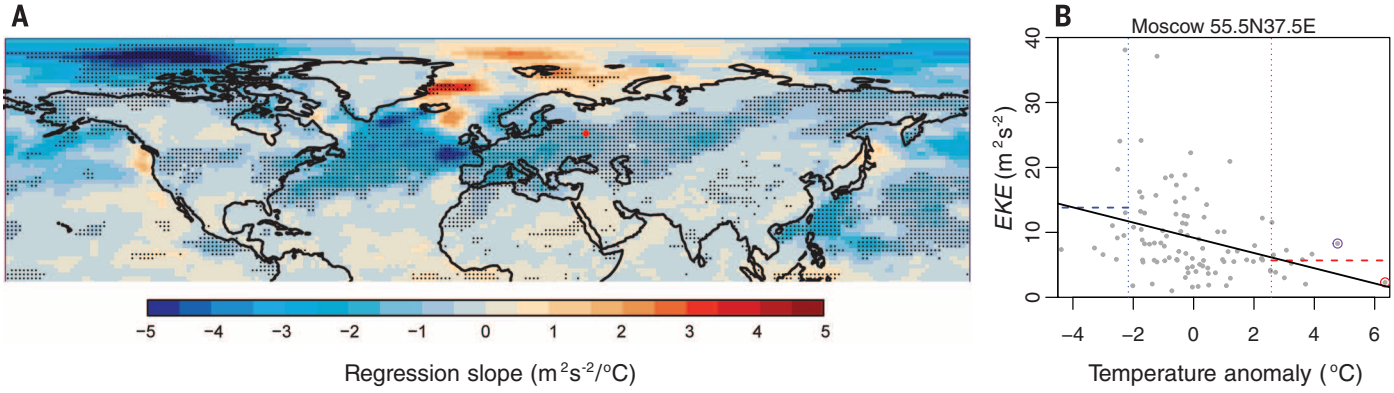

Fig. 4. Regression analysis between EKE and near-surface temperature during the summer months (June, July, and August). (**A**) Slope of the regression analysis. Both variables were linearly detrended, and stippling indicates significance at the 5% level. (**B**) EKE plotted against near-surface temperature anomaly for Moscow [red dot in (A)] for individual summer months, showing that the 10% coldest summer months (left of the vertical blue dotted line) have a substantially higher EKE (14 m^2/s^2; i.e., the horizontal blue dashed line) and the 10% warmest months (right of the vertical red dotted line) a substantially lower EKE (5.7 m^2/s^2; i.e., the horizontal red dashed line). Red and purple circles indicate, respectively, July and August 2010.

in kinetic energy, which is in good agreement with the bandpass-filtered results.

Wave 10 has seen a significant reduction in both amplitude and phase speed (Fig. 3A), which dropped respectively by –11% and –20% over the 1979–2013 period, with both negative trends acting to reduce EKE. A reduction in amplitude means lower wind speeds associated with weaker high- and low-pressure synoptic weather systems and thus lower EKE. A reduced phase speed implies more-persistent synoptic weather systems and fewer of them over the full season. The probability-density distribution of the wave period shows that wave periods in the EKE-relevant range (2.5 to 6 days) are dominated by wave 10 (fig. S21). During roughly half of all summer days, wave 10 had a wave period within this range. This suggests that the reduction in amplitude and phase speed of wave 10 contributed substantially to the reduction in EKE.

Summer EKE declined by 8 to 15% over the past decades, whereas the CMIP5 models project similar changes only by the end of the 21st century under a high-emission scenario (*24*). Either the climate models underpredict dynamical changes, or multidecadal variability played a role in the observed changes. In the other seasons, dynamics weakened as well, but here significant changes are only detected for the zonal-mean flow in autumn (SM text S3). Although the Arctic has warmed most in winter (*1*), the strongest changes in the meridional temperature gradient within the mid-latitudes occurred in summer, followed by autumn (fig. S17). Therefore, U_T and U itself weakened most in those seasons (fig. S17). The smaller year-to-year variability in those seasons (and especially in summer), as compared to winter, improves signal-to-noise ratios, making trend detection possible at an earlier stage (fig. S15). Likewise, variability in summer EKE is only half that of the other seasons (fig. S16B), and hence the signal-to-noise ratio is much larger for summer. In fact, summer EKE has weakened by more than two standard deviations over 1979–2013 (fig. S16C). Therefore, contrary to previous suggestions (*1*–*3*), the influence of Arctic amplification on mid-latitude weather is unlikely to be limited to autumn and winter only.

In summer, synoptic storms transport moist and cool air from the oceans to the continents, bringing relief during periods of oppressive heat. Low cyclone activity over Europe in recent years has led to more-persistent weather (*32*, *33*) contributing to prolonged heat waves. Regression analysis between EKE and near-surface temperature for summer months reveals that over mid-latitude continental regions, these quantities are negatively correlated (Fig. 4A). Thus, hot summer months are associated with low EKE (SM text S5). Over most of Eurasia and the United States, the negative regression slope is significant at the 5% level. In these storm track–affected regions, EKE in the 10% hottest months was only about half its summer climatological value (Fig. 4B and figs. S22 to S24). Low cyclone activity (and thus low EKE) imply that cool maritime air masses become less frequent, creating favorable conditions for the buildup of heat and drought over continents. This probably prolongs the duration of blocking weather systems, as, for example, during the Russian heat wave of 2010 (*18*, *34*). In particular, the record-breaking July temperatures over Moscow were associated with extremely low EKE (Fig. 4B).

Recent studies have emphasized the importance of quasi-stationary waves for summer heat extremes (*15*, *16*, *25*, *35*), showing that the frequency of wave-resonance events associated with high-amplitude quasi-stationary waves has increased since the onset of rapid Arctic amplification in 2000 (*16*). Here we show that the amplitude of fast-moving waves has steadily decreased, and also that the rate in this weakening seems to have increased since 2000 (fig. S25). Both of these observations are consistent with more-persistent summer weather (SM text S6). Low monthly EKE implies low weather variability within that month, indicating persistent weather conditions, consistent with quasi-stationary waves. The long-term reduction in EKE should lead to a reduction in weather variability on short time scales (less than a week), in agreement with the reduced intraseasonal daily temperature variance observed (*36*) and theoretical arguments (*37*). However, our results show that low EKE is associated with heat extremes on monthly time scales. Therefore, on such longer time scales, variability might actually increase due to a reduction in EKE. This seems consistent with Huntingford *et al.* (*38*), who report that the largest increase in interannual seasonal temperature variance occurred in the mid-latitude boreal summer. To test this hypothesis, studies are needed that quantify both interannual and intraannual variability on all relevant subseasonal time scales.

This study shows that boreal summer circulation has weakened, together with a reduction in the pole–to–mid-latitude temperature gradient. This has made weather more persistent and hence favored the occurrence of prolonged heat extremes.

REFERENCES AND NOTES

1. J. Cohen *et al.*, *Nat. Geosci.* **7**, 627–637 (2014).
2. D. Budikova, *Global Planet. Change* **68**, 149–163 (2009).
3. J. E. Walsh, *Global Planet. Change* **117**, 52–63 (2014).
4. R. L. Newson, *Nature* **241**, 39–40 (1973).
5. M. Warshaw, R. R. Rapp, *J. Appl. Meteorol.* **12**, 43–49 (1973).
6. J. A. Francis, S. J. Vavrus, *Geophys. Res. Lett.* **39**, L06801 (2012).
7. J. E. Overland, J. A. Francis, E. Hanna, M. Wang, *Geophys. Res. Lett.* **39**, L19804 (2012).
8. R. Jaiser, K. Dethloff, D. Handorf, A. Rinke, J. Cohen, *Tellus Ser. A Dyn. Meterol. Oceanogr.* **64**, 1–11 (2012).
9. J. L. Cohen, J. C. Furtado, M. A. Barlow, V. A. Alexeev, J. E. Cherry, *Environ. Res. Lett.* **7**, 014007 (2012).
10. F. Pithan, T. Mauritsen, *Nat. Geosci.* **7**, 181–184 (2014).
11. J. A. Screen, I. Simmonds, C. Deser, R. Tomas, *J. Clim.* **26**, 1230–1248 (2013).
12. E. A. Barnes, *Geophys. Res. Lett.* **40**, 4734–4739 (2013).
13. J. A. Screen, I. Simmonds, *Geophys. Res. Lett.* **40**, 959–964 (2013).
14. E. Kintisch, *Science* **344**, 250–253 (2014).
15. V. Petoukhov, S. Rahmstorf, S. Petri, H. J. Schellnhuber, *Proc. Natl. Acad. Sci. U.S.A.* **110**, 5336–5341 (2013).
16. D. Coumou, V. Petoukhov, S. Rahmstorf, S. Petri, H. J. Schellnhuber, *Proc. Natl. Acad. Sci. U.S.A.* **111**, 12331–12336 (2014).

17. J. A. Screen, *Environ. Res. Lett.* **8**, 044015 (2013).
18. S. Schubert, H. Wang, M. Suarez, *J. Clim.* **24**, 4773–4792 (2011).
19. J. Pedlosky, *Geophysical Fluid Dynamics* (Springer, New York, 1979).
20. K. Fraedrich, H. Böttger, *J. Atmos. Sci.* **35**, 745–750 (1978).
21. G. J. Boer, T. G. Shepherd, *J. Atmos. Sci.* **40**, 164–184 (1983).
22. M. Blackmon, *J. Atmos. Sci.* **33**, 1607–1623 (1976).
23. D. Coumou, V. Petoukhov, A. V. Eliseev, *Nonlinear Process. Geophys.* **18**, 807–827 (2011).
24. J. Lehmann, D. Coumou, K. Frieler, A. V. Eliseev, A. Levermann, *Environ. Res. Lett.* **9**, 084002 (2014).
25. H. Teng, G. Branstator, H. Wang, G. Meehl, W. M. Washington, *Nat. Geosci.* **6**, 1–6 (2013).
26. K. E. Trenberth, J. T. Fasullo, G. Branstator, A. S. Phillips, *Nat. Clim. Change* **4**, 911–916 (2014).
27. D. P. Dee *et al.*, *Q. J. R. Meteorol. Soc.* **137**, 553–597 (2011).
28. M. Murakami, *Mon. Weather Rev.* **107**, 994–1013 (1979).
29. J. Lu, G. Chen, D. M. W. Frierson, *J. Clim.* **21**, 5835–5851 (2008).
30. J. P. Peixoto, A. H. Oort, *Physics of Climate* (American Institute of Physics, New York, 1992).
31. T. Woollings, M. Blackburn, *J. Clim.* **25**, 886–902 (2012).
32. J. Kyselý, R. Huth, *Theor. Appl. Climatol.* **85**, 19–36 (2005).
33. J. Kyselý, *Global Planet. Change* **62**, 147–163 (2008).
34. R. Dole *et al.*, *Geophys. Res. Lett.* **38**, L06702 (2011).
35. J. A. Screen, I. Simmonds, *Nat. Clim. Chang.* **4**, 704–709 (2014).
36. J. A. Screen, *Nat. Clim. Chang.* **4**, 577–582 (2014).
37. T. Schneider, T. Bischoff, H. Plotka, *J. Clim.* **28**, 2312–2331 (2014).
38. C. Huntingford, P. D. Jones, V. N. Livina, T. M. Lenton, P. M. Cox, *Nature* **500**, 327–330 (2013).

ACKNOWLEDGMENTS

We thank the CMIP5 climate modeling groups and the European Centre for Medium-Range Weather Forecasts and NCEP-NCAR for making their model and reanalysis data available. Comments by three anonymous reviewers, S. Rahmstorf, and P. Eickemeier have considerably improved the manuscript. Data presented in this manuscript will be archived for at least 10 years by the Potsdam Institute for Climate Impact Research. The work was supported by the German Research Foundation (grant no. CO994/2-1) and the German Federal Ministry of Education and Research (grant no. 01LN1304A). D.C. designed the research; D.C., J.L., and J.B. performed the analysis; and D.C., J.L., and J.B. wrote the manuscript.

SUPPLEMENTARY MATERIALS

www.sciencemag.org/content/348/6232/324/suppl/DC1
Text S1 to S6
Figs. S1 to S25
Table S1
References
Data Deposition

26 September 2014; accepted 26 February 2015
Published online 12 March 2015;
10.1126/science.1261768

ICE SHEETS

Volume loss from Antarctic ice shelves is accelerating

Fernando S. Paolo,[1]* Helen A. Fricker,[1] Laurie Padman[2]

The floating ice shelves surrounding the Antarctic Ice Sheet restrain the grounded ice-sheet flow. Thinning of an ice shelf reduces this effect, leading to an increase in ice discharge to the ocean. Using 18 years of continuous satellite radar altimeter observations, we have computed decadal-scale changes in ice-shelf thickness around the Antarctic continent. Overall, average ice-shelf volume change accelerated from negligible loss at 25 ± 64 cubic kilometers per year for 1994–2003 to rapid loss of 310 ± 74 cubic kilometers per year for 2003–2012. West Antarctic losses increased by ~70% in the past decade, and earlier volume gain by East Antarctic ice shelves ceased. In the Amundsen and Bellingshausen regions, some ice shelves have lost up to 18% of their thickness in less than two decades.

The Antarctic Ice Sheet gains mass through snowfall and loses mass at its margin through submarine melting and iceberg calving. These losses occur primarily from ice shelves, the floating extensions of the ice sheet. Antarctica's grounded-ice loss has increased over the past two decades (*1*, *2*), with the most rapid losses being along the Amundsen Sea coast (*3*) concurrent with substantial thinning of adjoining ice shelves (*4*, *5*) and along the Antarctic Peninsula after ice-shelf disintegration events (*6*). Ice shelves restrain ("buttress") the flow of the grounded ice through drag forces at the ice-rock boundary, including lateral stresses at sidewalls and basal stresses where the ice shelf rests on topographic highs (*7*, *8*). Reductions in ice-shelf thickness reduce these stresses, leading to a speed-up of ice discharge. If the boundary between the floating ice shelf and the grounded ice (the grounding line) is situated on a retrograde bed (sloping downwards inland), this process leads to faster rates of ice flow, with potential for a self-sustaining retreat (*7*, *9*, *10*).

Changes in ice-shelf thickness and extent have primarily been attributed to varying atmospheric and oceanic conditions (*11*, *12*). Observing ice-shelf thickness variability can help identify the principal processes influencing how changing large-scale climate affects global sea level through the effects of buttressing on the Antarctic Ice Sheet. The only practical way to map and monitor ice-shelf thickness for this vast and remote ice sheet at the known space and time scales of ice-shelf variability is with satellite altimetry. Previous studies have reported trends based on simple line fits to time series of ice-shelf thickness (or height) averaged over entire ice shelves or broad regions (*4*, *13*) or for short (~5-year) time intervals (*5*, *14*, *15*). Here, we present a record of ice-shelf thickness that is highly resolved in time (~3 months) and space (~30 km), using the longest available record from three consecutive overlapping satellite radar altimeter missions (ERS-1, 1992–1996; ERS-2, 1995–2003; and Envisat, 2002–2012) spanning 18 years from 1994 to 2012.

Our technique for ice-shelf thickness change detection is based on crossover analysis of satellite radar altimeter data, in which time-separated height estimates are differenced at orbit intersections (*13*, *16*, *17*). To cross-calibrate measurements from the different satellite altimeters, we used the roughly 1-year overlap between consecutive missions. The signal-to-noise ratio of altimeter-derived height differences for floating ice in hydrostatic equilibrium is roughly an order of magnitude smaller than over grounded ice, requiring additional data averaging to obtain comparable statistical significance. We aggregated observations in time (3-month bins) and space (~30-km cells). Because the spatial distribution of crossovers changes with time (due, for example, to nonexact repeat tracks and nadir mispointing), we constructed several records at each cell location and stacked them in order to produce a mean time series with reduced statistical error (*18*). We converted our height-change time series and rates to thickness changes by assuming that observed losses occurred predominantly at the density of solid ice (basal melting) (*4*, *5*, *17*). This is further justified by the relative insensitivity of radar measurements to fluctuations in surface mass balance (*18*). For volume changes, we tracked the minimum (fixed) area of each ice shelf (*18*). We assessed uncertainties for all estimates using the bootstrap approach (resampling with replacement of the residuals of the fit) (*19*), which allows estimation of formal confidence intervals. All our uncertainties are stated at the 95% confidence level [discussion of uncertainties are provided in (*18*) and the several corrections applied are stated in (*20*)].

We estimated 18-year trends in ice-shelf thickness by fitting low-order polynomials (degree $n \leq 3$) to the data using a combination of lasso regularized-regression (*21*) and cross-validation for model-parameter selection (the shape of the fit is determined by the data). This combined approach allowed us to minimize the effect of short-term variability on the 18-year trends. Relative to previous studies (*4*, *5*, *13*, *22*), we have improved estimations by (i) using 18-year continuous records, (ii) implementing a time series averaging

[1]Scripps Institution of Oceanography, University of California, San Diego, CA, USA. [2]Earth & Space Research, Corvallis, OR, USA.
*Corresponding author. E-mail: fpaolo@ucsd.edu

The weakening summer circulation in the Northern Hemisphere mid-latitudes

Dim Coumou *et al.*

Science **348**, 324 (2015);
DOI: 10.1126/science.1261768